

AD No. 27 369  
ASTIA FILE COPY

THE UNIVERSITY OF CHICAGO  
DEPARTMENT OF METEOROLOGY

ON THE MEAN THERMAL STRUCTURE  
OF TROPICAL CYCLONES

and

SHIP REPORTS OF CLOUDINESS AS AN AID  
IN LOW LATITUDE ANALYSIS

Reports on Research

Prepared under Contract No. N6ori-02036

Project NR 085 003

Office of Naval Research

March 1954

# On the Mean Thermal Structure of Tropical Cyclones

by

Charles L. Jordan and Elizabeth L. Jordan

The University of Chicago<sup>1</sup>

## Abstract

Radiosonde ascents made within the circulation of hurricanes are combined to arrive at the mean temperature and pressure-height distribution about the storm. The results are compared with a thermodynamic model of the tropical storm, with the mean wind field and with two individual case studies of intense tropical cyclones.

\* \* \*

## Introduction

Aerological ascents in tropical storms have made possible quite detailed descriptions of the three dimensional thermal structure of the rain area -- the central core of wind and weather -- and, to a lesser extent, the eye of the storm (c.f. Riehl, 1951; 1954). The thermal model described by Riehl was arrived at by considering representative features of soundings made in tropical cyclones rather than through a statistical procedure of combining aerological data into mean soundings. It is the purpose of this paper to present such aerological data for the hurricane and to compare it with (a) the mean wind field in tropical storms (E. S. Jordan, 1952), (b) the thermal structure deduced by Riehl (1951), and (c) selected individual cases.

## Mean Aerological Data

A total of about 300 radiosonde ascents made within 6° lat. of the center of mature hurricanes in the Atlantic-Caribbean-Gulf of Mexico area during the years 1946-1952 form the basic data for this study. Reports north of 35°N were excluded as well as those taken in the circulation of storms which had completed recurvature.

The height, temperature and dew point were tabulated for each mandatory pressure surface along with the distance of the station from the storm center and the angle between the direction of motion of the storm and a line joining the station and storm center.

The fact that radiosonde ascents are more likely to be made in weak storms rather than in severe ones is a consideration in the interpretation of the results. Also, the seasonal change in the position of the mean storm tracks is such that the distribution of data, relative to the storm, is not completely random in space and time. For example, much of the data to the

---

<sup>1</sup>This paper has been prepared under research contracts between the Office of Naval Research and The University of Chicago.

left of the storm tracks came from Puerto Rico, eastern Cuba and the east coast of the United States in storms which recurved along the east coast. In contrast, much of the data to the right of the storm tracks came from western Cuba and Gulf coast stations during Caribbean and Gulf storms which have a different seasonal distribution from those in the Atlantic. In view of these difficulties we must be careful in attributing significance to minor features which may be merely reflection of the non-homogeneous character of the data.

Mean temperature: The mean temperature values for the various mandatory levels were obtained by grouping and averaging all temperature data in concentric rings one degree latitude wide measured from the center of the storm. The number of observations in each ring and at each level is shown in Table I. The few reports within  $1^{\circ}$  lat of the storm center have not been included.

Table I. Number of observations used for the means shown in Table II.

Dist. from Center in $^{\circ}$ lat.	$1^{\circ}$ - $2^{\circ}$	$2^{\circ}$ - $3^{\circ}$	$3^{\circ}$ - $4^{\circ}$	$4^{\circ}$ - $5^{\circ}$	$5^{\circ}$ - $6^{\circ}$
Surface	27	40	58	81	87
850 mb	27	41	58	82	89
700	27	41	58	81	89
500	23	40	56	78	83
400	21	39	54	77	81
300	31	35	49	77	81
200	18	31	45	73	73
150	15	27	34	59	59
100	10	12	20	44	41
50	3	7	9	20	23

Mean soundings were prepared from the temperature data given in Table II. The soundings for the inner ring ( $1^{\circ}$  -  $2^{\circ}$  lat) and the outer ring ( $5^{\circ}$  -  $6^{\circ}$  lat) are shown in Fig. 1. The temperature distribution near the surface is quite uniform and the warm core characteristics of the hurricane center become marked only at the levels above 700 mb. The temperature difference between the inside and outside ring increases from essentially zero near the surface to a maximum of over  $2^{\circ}\text{C}$  near 300 mb and then decreases with a reversal occurring below 100 mb. This difference is quite small in comparison with that observed in an intense tropical storm where the inside may be as much as  $10^{\circ}\text{C}$  warmer than the outside (Kasahara, 1953). In the lower stratosphere -- tropopause to 70 mb -- the outer ring is the order of  $2^{\circ}$  -  $4^{\circ}\text{C}$  warmer than the inner ring.

Table II. Mean Temperature ( $^{\circ}\text{C}$ )

Dist. from Center in $^{\circ}$ lat.	1 $^{\circ}$ -2 $^{\circ}$	2 $^{\circ}$ -3 $^{\circ}$	3 $^{\circ}$ -4 $^{\circ}$	4 $^{\circ}$ -5 $^{\circ}$	5 $^{\circ}$ -6 $^{\circ}$
Surface	25.7	25.7	25.8	26.3	26.3
850 mb	17.3	17.1	17.2	17.4	17.3
700	9.4	9.2	8.9	8.8	8.9
500	-4.6	-5.1	-5.9	-6.0	-6.2
400	-14.8	-15.0	-16.0	-16.5	-16.9
300	-29.4	-30.3	-31.0	-31.3	-31.9
200	-51.6	-52.4	-52.9	-52.9	-53.7
150	-65.6	-66.3	-66.5	-66.1	-66.4
100	-75.1	-75.3	-73.2	-72.8	-72.1
50	-59.7	-62.6	-59.0	-58.2	-57.0

At the beginning of this investigation the temperature data was further divided into quadrants and mean values were determined for each quadrant of each ring. The differences between quadrants were not sufficiently large to warrant presentation. However it was evident that in the outer portion of the storm the mean temperature of the quadrants to the right of the direction of motion was warmer throughout the troposphere -- roughly  $0.5^{\circ}\text{C}$  -- than the corresponding areas to the left of the storm. It cannot be established whether this asymmetry is a significant feature of the storm circulation or whether it has been introduced by the general current in which the storm is moving. If we accept the latter it can be interpreted as an indication that hurricanes move in a current of slight baroclinity.

Mean tropopause structure: The tropopause was determined by plotting the upper portion of all soundings on thermodynamic diagrams. Most soundings showed a steep lapse rate in the upper troposphere and a sharp tropopause. In the questionable cases the tropopause was taken at the level (above 200 mb) at which the largest change in lapse rate occurred. A disproportionately large percentage of the tropopauses were shown exactly at the 150 and 100 mb mandatory levels. Consequently, these values were not used in computing the tropopause data shown in Table III. The general features shown by the data in Table III are an increase of the height of the tropopause toward the central portion of the storm, a progressive decrease in temperature with increase of tropopause height and a fairly constant potential temperature.

Table III. Mean Pressure, Height, Temperature and potential temperature at the Mean Tropopause Level

Dist. from Center in ° lat.	1°-2°	2°-3°	3°-4°	4°-5°	5°-6°
Pressure (mb)	115	118	123	127	127
Height (ft)	51,880	51,330	50,570	49,920	49,870
Temperature (°C)	-77.2	-76.6	-74.7	-73.6	-73.5
Pot. Temp. (°A)	364	363	363	362	362

Mean pressure-height data: The mean surface pressure and the mean height of the various standard isobaric surfaces for each ring are shown in Table IV. These were determined by averaging the individual reported values. Height values were also computed from the mean soundings beginning with the averaged 1000 mb heights. In general, agreement between the two sets of height data was good and either could have been used for the following discussion. Most of the individual differences were 20 ft or less; the largest values, up to 40 ft, appeared at the 100 mb level where the number of observations was quite small (Table I).

Table IV. Mean surface pressure (mb) and heights of standard isobaric surfaces (tens of ft)

Dist from Center in ° lat.	1°-2°	2°-3°	3°-4°	4°-5°	5°-6°
Surface	1005.0	1006.6	1008.6	1009.7	1011.6
850 mb	482	490	495	497	503
700	1020	1024	1032	1034	1039
500	1913	1916	1923	1924	1928
400	2479	2486	2488	2489	2492
300	3173	3173	3176	3176	3178
200	4079	4080	4079	4077	4075
100	5448	5448	5450	5454	5450

The radial height gradient (Fig. 2) decreases slowly up to 400 mb and fairly rapidly above this level. At 200 mb the greatest height value is in

the  $2^{\circ} - 3^{\circ}$  lat ring with decreases both inward and outward. This height distribution is consistent with the mean wind distribution (E. S. Jordan, 1952) since the streamline patterns at 40,000 and 45,000 ft showed an inner cyclonic core surrounded by anticyclonic circulation. The magnitude of the geostrophic wind and the vertical shear indicated by Fig. 2 also compare favorably with the mean wind distribution.

The mean height gradient across the storm normal to the direction of motion ( $\Delta H_n$ ) was found by averaging the reported height values from the  $4^{\circ} - 6^{\circ}$  lat ring in the quadrants  $45^{\circ} - 135^{\circ}$  to the right and to the left of the direction of motion (Fig. 3). This was converted to geostrophic speed ( $U_{gs}$ ) assuming a mean latitude of  $25^{\circ}$  (Table V). An average of all tropospheric values, after weighting each value for the pressure interval it represents, is equivalent to a geostrophic speed of 10-11 knots. This agrees closely with the average speed (9.7 knots) arrived at by considering the variation of the strength of the mean wind across the storm from the surface to 300 mb (E. S. Jordan, 1952).

Table V. Mean geostrophic components across storm: acting along direction of motion ( $U_{gs}$ ) and to the right of the direction of motion ( $U_{gn}$ ).

	850 mb	700 mb	500 mb	400 mb	300 mb	200 mb	100 mb
$U_{gs}$ (knots)	3	5	8	12	13	19	7
$U_{gn}$ (knots)	9	7	4	-6	-2	-2	1

Also the mean height gradient along the direction of motion ( $\Delta H_s$ ) was obtained for the  $4^{\circ} - 6^{\circ}$  quadrant sectors centered about the direction of motion (Fig. 3). The height gradient was such that the resulting geostrophic wind ( $U_{gn}$ ) is directed to the right of the direction of motion at low levels and to the left at upper levels (Table V). Averaging over the troposphere gives a magnitude of 2 - 3 knots directed to the right of the direction of motion. The results of the above calculations when combined with the mean wind study suggests the following conclusion: The storm moves with the mean flow in which it is imbedded, but this direction is some  $10^{\circ} - 15^{\circ}$  to the right of that indicated by geostrophic calculations. It would appear that the particular level at which the geostrophic wind would, in the mean, be the best approximation to the storm movement is found in the vicinity of 450 mb.  $U_{gs}$  at this level is very nearly equal to the mean storm speed and  $U_{gn}$  has a zero in this vicinity.

Mean moisture: The results obtained by averaging the dew points were quite disappointing and no quantitative use has been made of them. The air near the storm center showed greater moisture content than the outside but differences were rather small. For example, the mean relative humidity increased from 80 to 85 percent at the surface, from 50 to 75 percent at 700 mb and from 35 to 45 percent at 300 mb.

The result of this calculation is attributed to the erratic behavior of the electrolytic hygrometer in heavy rain. Quite low humidity values can result from the "washing out" effect mentioned by Middleton and Spilhaus (1953). The inclusion of a relatively small number of very "dry" soundings

can lead to mean humidity values which are appreciably low. Since the moisture normally varies over a large range, it is much more difficult to detect and eliminate errors in dew point than in temperature. Temperature errors of  $5^{\circ}\text{C}$  are quite apparent but dew point errors of even  $10^{\circ}\text{C}$  may not be detectable.

A systematic error in the moisture of the type indicated above would contribute toward low pressure-height values near the storm center. The maximum possible errors, roughly 40 ft, would effect only a small percentual change in the height gradient up to 400 mb (Table IV), but would be more important in the upper troposphere where the gradients are weaker. This effect could contribute toward a reversal of the inward directed height gradient at a slightly lower level than shown in Fig. 2 but the qualitative result would remain unchanged.

In view of the moisture uncertainties we will assume in the following that the inner core of the storm is saturated in a deep layer above the cloud bases. This is hardly an assumption since aircraft reconnaissance reports in most well-developed storms show continuous cloud even within the areas between radar bands. In the outer regions where the radar bands are more widely spaced there is undoubtedly appreciable horizontal variation in the relative humidity.

#### Maintenance of the Thermal Field

In the previous section we have discussed the general features of the thermal structure of the hurricane shown by the mean soundings. Now we will examine in more detail the thermal field in relation to thermodynamic processes and the vertical circulation within the storm. In order to facilitate the qualitative arguments which follow we will assume that the vertical circulation within the hurricane is of the form deduced by Riehl (1951) (Fig. 4). Further on we will point out some minor modifications of this model suggested by our data; however, the essential features remain unchanged.

The pertinent features of the thermal field can be brought out more clearly by treating the mean values of Table II as anomalies from the mean tropical atmosphere<sup>2</sup>. The deviations of the mean hurricane soundings from the mean tropical have been plotted in the form of a radial cross section (Fig. 5). Perhaps the most striking feature of this figure is the fact that the hurricane is only a little warmer than mean conditions throughout much of the circulation. However in the upper troposphere the anomalies become marked and the storm influence extends over a very large area. The analysis of the anomaly distribution has not been extended above 150 mb because of the complications in the vicinity of the tropopause. The five mean hurricane soundings and the mean tropical pass very close to the intersection of 125 mb and  $-74^{\circ}\text{C}$ . This isopycnic level as well as the anomaly pattern in this region may have little significance and may represent somewhat fictitious results brought about by the averaging technique used in determining the mean tropopause values.

The vertical temperature distribution of rising air parcels within the  $1^{\circ} - 2^{\circ}$  lat ring can be described by an adiabatic ascent curve if saturation above the cloud bases is assumed. Curve a, Fig. 6 shows the temperature

---

<sup>2</sup>The "mean tropical atmosphere" or "mean tropical conditions" will in all cases refer to the mean nighttime sounding computed by Schacht (1946).



distribution beginning with the mean surface characteristics (Table II, IV) and assuming the cloud bases at 1000 ft. The deviation of this curve from the mean tropical (dashed curve, Fig. 6) shows a somewhat different anomaly distribution from that shown for the inner ring in Fig. 5, especially in the vicinity of the upper tropospheric maximum. The vertical anomaly distribution in Fig. 5 can, however, result from parcel ascent provided the trajectories have a radial component. Anomalies of the correct magnitude for the 200 - 300 mb maximum could result from parcel ascents starting within the  $1^{\circ}$  lat radius at reduced surface pressures. For example, curve b of Fig. 6 illustrates a parcel ascent using the cloud bases at 1000 ft and a rather low surface pressure of 970 mb. However, the same upper temperature distribution could be realized with a higher surface pressure if the cloud bases were lower; for example, 990 mb and 500 ft. Thus the observed anomaly distribution is consistent with parcel ascent provided the motion has an outflow component as indicated in Fig. 4. A radial outflow of this type has been detected from the mean wind distribution (E. S. Jordan, 1952). It was established that, in the mean, the outflow first becomes significant above 30,000 ft, attains a maximum of the order of 15 knots in the vicinity of 40,000 ft and decreases to about 10 knots at 45,000 ft. Such a pattern of outflow is consistent with the eye boundary slope required by the surface pressure distribution (Haurwitz, 1935).

The parcel technique can also be used in the upper outflow region to determine roughly the ratio of the horizontal to the vertical motion. For example, if we assume that the air ascends moist adiabatically from 300 mb in the  $1^{\circ}$  -  $2^{\circ}$  lat ring (Fig. 1, point A) it would arrive at 200 mb with the observed temperature of the  $5^{\circ}$  -  $6^{\circ}$  lat ring (Fig. 1, point B). From this reasoning, the rising air moves outward  $4^{\circ}$  lat while rising approximately 10,000 ft. Thus the mean slope of the ascending branch of the circulation, as well as the eye boundary, is indicated to lie near the vertical below 300 mb and to be of the order of 1:125 in the 300 - 200 mb layer.

We have been unable to find conclusive evidence of the eye boundary which is shown in Fig. 4 as the zone of separation between the inflow and outflow. An attempt to determine the eye boundary from individual soundings met with little success. A fair proportion of the inner soundings did show stable layers in the region 400 - 200 mb but these were not regular enough that quantitative use could be made of them. Again, as in the case of the tropopause, a large percentage of the lapse rate changes occurred at the mandatory levels. The eye boundary is, of course, quite fluid and mixing must take place across it. Perhaps we have not been able to find such a zone simply because it does not exist as a steady state feature, particularly in the outer zone.

The following remarks can be made concerning the structure indicated by Fig. 4 and that shown by the mean hurricane data: (a) The upward slope of the tropopause toward the center, shown by Fig. 4, is verified but no evidence was found for a double structure; however, our data did not extend all the way into the center. (b) The tropopause heights for the hurricane are about 1 km lower than indicated by Fig. 4, but the mean data is somewhat biased toward the weaker storms. (c) The following horizontal scale for Fig. 4 is suggested. The region of greatest curvature of the eye boundary should be placed about  $1.5^{\circ}$  lat from the center and the total radial extent should be of the order of  $6^{\circ}$  lat. (d) The eye boundary in the upper troposphere is quite weak and may not exist as a steady state feature of the circulation.

Our primary concern has been with the inner core of ascent and the upper



outflow layer. These we visualize as the active components of the circulation and the features of primary significance in the maintenance of the storm. Much of the outer circulation is considered to be somewhat passive and the temperature anomalies are sufficiently small so that merely the proximity to the storm center is an adequate explanation for their existence. The absence of any large temperature anomalies in the lower troposphere, even as far out as  $60^\circ$  lat, offers strong support for the idea that the compensating subsidence must take place at distances far removed from the storm center (Riehl, 1951). The large areal extent of the increased anomalies in the upper troposphere is thus taken as evidence that the outflow layer does transfer heat for great distances before losing it to the outside. This dispersal of the descending branch of the circulation over an immense area points to the necessity of an open system treatment in any complete hurricane theory.

### Case Studies

Case studies of tropical cyclone structure have been rather infrequent since aerological stations are usually widely spaced in the tropics and since operations are often interrupted by the storm. However, Palmén (1948) using special upper air data from Miami, Florida for a four day period arrived at a rather detailed vertical cross-section of a hurricane. Several other studies (cf. Simpson, 1947; Arakawa, 1950) have combined data from one or more aerological stations to arrive at various types of cross-sections of tropical storms.

The data presented below demonstrate that the general features brought out by the mean data are also quite evident in individual cases. Differences are mainly in the intensity shown by various attributes of the storm and in the appearance of smaller scale features. Although the microstructure is well-marked, these features show little continuity between successive soundings and therefore are not effective in obscuring the general storm features shown by the mean data.

Bermuda - September 4-7, 1953: A relatively large hurricane moved on a slowly recurving path west of Bermuda during the period Sept. 4-7, 1953 (Fig. 7). The storm center did not come closer to the station than about 200 miles. Skies were broken to overcast with stratus and stratocumulus with brief light showers; surface winds were 25-30 knots and gusty during the passage. An unusually complete set of soundings, taken at three hourly intervals over a 30 hour period, was obtained by the rawinsonde station at Kindley AFB, Bermuda.

The time section of the wind field (Fig. 8) shows the general features discussed previously but, in addition, a great deal of microstructure. The wind direction in most cases shows a general anticyclonic turning of the order of  $20^\circ - 30^\circ$  in the layer surface to 30,000 ft. Above 30,000 ft the turning is much more rapid and at the 45,000 and 50,000 ft levels the flow is almost completely opposite to that observed at the low levels. This is shown more clearly by plotting all 50,000 ft winds together (Fig. 9); each wind being placed at the proper distance and orientation from the storm center (center of diagram). The dashed winds were observed within the same storm circulation at San Juan, Puerto Rico on Sept. 3 and 4.

The maximum wind speeds were found in the lower 10,000 ft and the vertical decreases were fairly weak below 20,000 ft. Surface effects were quite pro-

nounced during the period of strongest winds. Speeds increased from 25-30 knots at the surface to 50-80 knots in the 4000-10,000 ft layer. The storm was nearest the station and the surface pressure lowest at about 06-00<sup>3</sup>. At this time the 40,000 and 45,000 ft winds indicate anticyclonic circulation; however, earlier winds suggest that the station was within the inner cyclonic core up to 40,000 ft at 05-21 and up to 45,000 ft at 05-18. The rapid turning of the 40,000 ft winds from southerly to northerly during Sept. 6 clearly suggests an eddy structure of the type drawn in the mean wind study (E. S. Jordan, 1952).

The height and temperature data have been plotted in time section form in Fig. 10. The height values show considerable variability, but the field of 24-hour height change shows a rather well-defined pattern. The fall center passes at about the same time at all levels and has a magnitude varying from a maximum of 250 ft at 1000 mb to a minimum of 150 ft at 500 and 400 mb. The anticyclonic turning of the wind in the layer 20,000 - 40,000 ft reached a minimum during the period of largest height falls.

The deviation of the 500-200 mb mean temperature<sup>4</sup> from the mean tropical showed considerable variation during the period the storm was within 5° lat of the station. The plot of this deviation versus the distance from the storm center (Fig. 11, light curve) shows that the upper troposphere was appreciably warmer than the mean hurricane case (heavy curve, Fig. 11) and the warm air extended over a larger area. Mean temperatures for lower layers also showed a general pattern similar to the 500-200 mb layer but the magnitude of the warming and the area affected were smaller. For example, the 500-700 mb deviation values varied from roughly -1.5°C to +2.0°C and all deviations greater than +1.0°C were within 4° of the storm center. The more pronounced warming in this case, in comparison with the mean hurricane results, is not surprising since the storm was quite intense--central pressure about 950 mb--and the circulation was large--5°-6° lat in radius. The relatively low deviation values shown at about the time the storm was nearest the station do not fit the model given by the mean hurricane results. Since there were three values, all from nighttime soundings, they cannot be easily neglected or attributed to diurnal effects. Perhaps these values should be accepted as evidence that appreciable microstructure is present within the hurricane either in the form of small scale moving disturbances or in the form of larger scale asymmetrical features.

The plotted soundings failed to show any definite evidence of the eye boundary but this is not surprising considering the distance from the storm center. Several soundings had stable layers or inversions at or below 400 mb and in most cases an upward decrease of moisture was present. Little continuity for the stable layers existed between the three-hourly soundings; consequently, these have been considered as microstructure rather than evidence for an organized descent in the lower levels in the outer portion of the storm. Only three of the eleven three-hourly soundings reached the 100 mb level so that little information was gained in respect to the character of the tropopause

---

<sup>3</sup>Sept. 6, 0000 GCT. This notation will be used hereafter for date and Greenwich time.

<sup>4</sup>Computed from the 500-200 mb thickness values.

and its variation in different portions of the storm. The three soundings which did reach the tropopause were quite different. One taken at 05-21, about the time of lowest pressure, had a definite tropopause at 108 mb,  $-74^{\circ}\text{C}$ . For comparison, the  $3^{\circ}$ - $4^{\circ}$  ring mean sounding shows the tropopause at  $-75^{\circ}\text{C}$  but at an appreciably higher pressure, 123 mb. The other two soundings showed a more complicated structure with stable layers below the level of minimum temperature.

The large scale features of the hurricane shown by the Bermuda data also stand out in the mean results. This consistency is especially marked in the close correspondence between the wind field and the thermal structure of the storm. This case study therefore offers support to the idea that the mean fields of wind and temperature are realistic and that the broad features of the hurricane can be approximated closely by the mean results.

Okinawa - August 16-19, 1951: An intense typhoon described by Simpson (1952) passed near Okinawa on Aug. 17-18, 1951 (Fig. 12). A total of eight radiosonde ascents were available from Kadena AFB, Okinawa during the period this storm was within  $6^{\circ}$  lat of the station. Two of these were made closer than  $2^{\circ}$  lat from the center and an eye dropsonde was made about the time the lowest pressure was recorded at the station. This series is much less complete than the Bermuda case; winds were entirely missing throughout the period of primary interest and the radiosonde ascents, made at six-hour intervals, were not available for all observation hours.

The surface reports showed that the station was within the area of heavy cloudiness and rain for nearly three days but most of the soundings were made on Aug. 16 and 17 prior to the arrival of the central core of weather. The minimum pressure (about 960 mb) was reported at 18-00 when the center was less than  $1^{\circ}$  lat to the east of the station. A dropsonde into the eye at about this time reported a central pressure of 935 mb. The maximum reported surface wind was 65 knots; however, reconnaissance aircraft reported winds in excess of 75 knots over a 150 mile radius. The possibility of a marked reduction in the surface wind at the station, such as noted in the Bermuda case, is clearly suggested.

The circulation of this typhoon covered a much larger area than attained by hurricanes. The intensity and size are reflected in Fig. 13 which shows the large warming which occurred as the storm approached. The upper troposphere temperatures shown by the 17-15 sounding, made roughly  $1.2^{\circ}$  lat from the center, are  $6^{\circ}$ - $10^{\circ}\text{C}$  warmer than those given by the 17-15 sounding located about  $6^{\circ}$  lat from the storm center. Comparison with mean tropical conditions is somewhat misleading since the ascents made just prior to the storm were considerably warmer than this mean sounding. However, a plot of the 500-200 mb mean temperature deviation (Fig. 14) facilitates comparison with the Bermuda case (Fig. 11). It is surprising, in view of the larger size of the typhoon at the surface, that the upper level warming began at a greater distance in the Bermuda series. The rate of warming and total temperature rise are considerably greater in the present case; however, the innermost sounding ( $1.2^{\circ}$  lat) is much closer to the storm center. The warming at lower levels is less, as shown for the 700 - 500 mb layer in Fig. 15, but parallels quite closely the 500 - 200 mb curve (Fig. 14). The beginning of the warming early on August 16 occurred at about the same time in both layers in contrast to the Bermuda results which showed large rises in the upper layer considerably before they appeared below. The greater consistency between successive observations in Fig. 14 and 15 in comparison with Fig. 10 is perhaps illusory since the frequency of soundings is so much less.

The soundings in general did not extend high enough so that the tropopause structure can be compared with previous results. The three soundings in Fig. 13 made nearest the storm center taken together show some evidence of a sloping eye boundary of the type drawn in Fig. 4. However, if the top of the stable layer at 480 mb on the 17-15 sounding is taken as the inside boundary of the mixing zone between the eye and the weather core of the storm, a quite shallow slope of 1:12 is indicated between the surface and this level. This slope was computed by taking the distance to the storm center as 75 miles (Fig. 12) and using the eye radius of 25 miles reported by the aircraft reconnaissance. However, after considering inaccuracies in the reported storm position and estimates of the eye size and the fact that the balloon may have drifted in toward the center 10-15 miles during its ascent to 480 mb, it is apparent that the computed slope may be appreciably in error. A weak stable layer, top at 300 mb, is found on the 17-03 sounding and a somewhat more distinct one is found at 275-265 mb on the 16-21 sounding. The ascents made at greater distances from the storm center showed no further evidence of the stable layer in the 300-200 mb region. The stable layer given by the three soundings shows a progressive decrease in elevation as the storm moves toward the station. If it can be assumed that this layer existed as a steady state feature an inclination of the order of 1:100 is indicated between the 16-21 and 17-03 soundings and 1:50 between the 17-03 and 17-15 ascents. These values appear consistent with the eye boundary slope drawn in Fig. 4 if the horizontal scale suggested by the mean hurricane data is used.

The case studies presented here represent very intense tropical storms while the mean data, as pointed out previously, are biased toward weaker storms. Nevertheless the major features shown by both the Atlantic and Pacific cases are quite consistent with the mean results. This is particularly marked at the upper tropospheric levels where it is apparent from all three sets of data that a very large area is affected by the storm. The area of the lower circulation may vary over a large range but the scale of the upper circulation is much less variable. Apparently the upper circulation serves an important role as a dispersal mechanism for the heat funneled upward near the storm center, and in this manner may exert appreciable influence on the large scale features of the planetary circulation.

#### Acknowledgment

The authors wish to express their appreciation to Dr. Herbert Riehl for his advice and criticism in the preparation of this report.

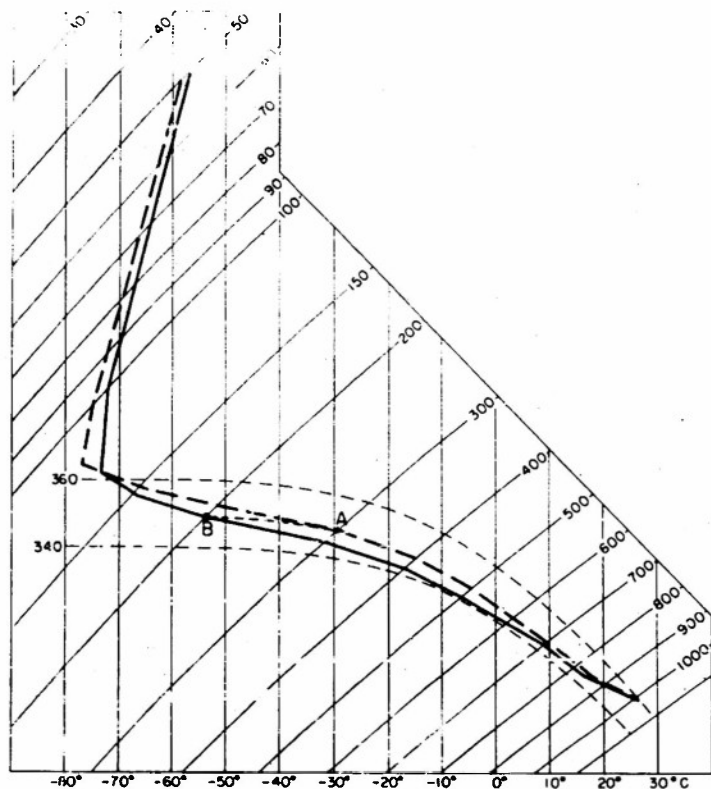


Fig. 1 Tephigram showing mean hurricane soundings for 1° - 2° lat (dashed) and 5° - 6° lat (solid).

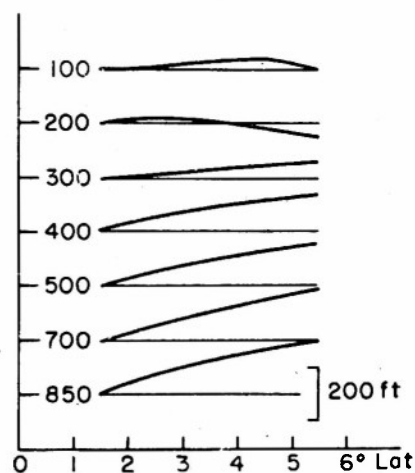


Fig. 2 Radial height profiles for standard isobaric surfaces.

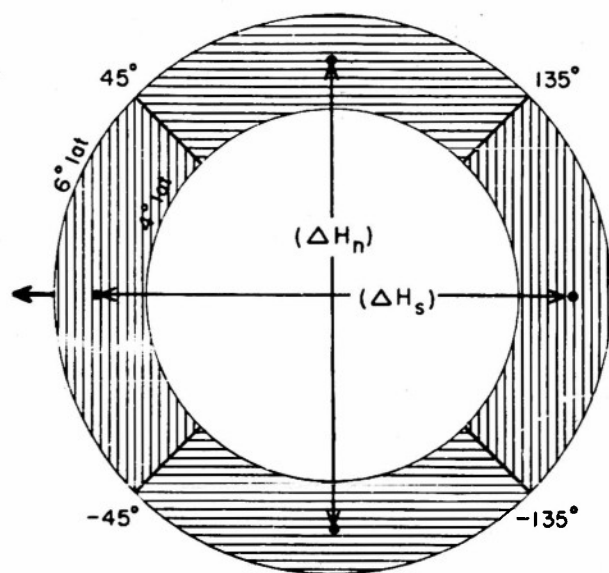


Fig. 3 An illustration showing the sectors used in computing the geostrophic components along and normal to the direction of motion of the storm. The direction of motion is along the heavy arrow.

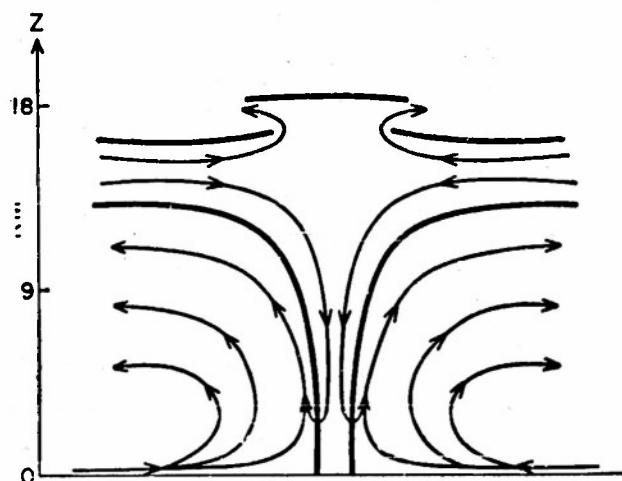


Fig. 4 Vertical cross section through mature tropical storm showing hypothetical model of the vertical circulation. Heavy solid lines are eye boundaries and tropopause (From Riehl, 1951.)



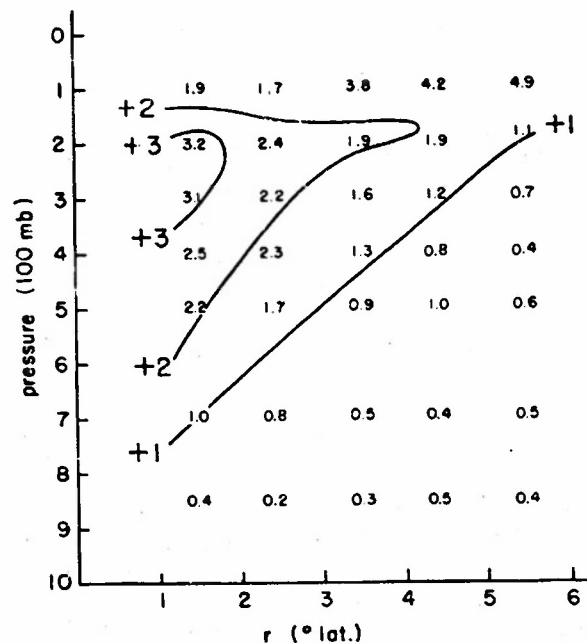


Fig. 5 Vertical cross section of the deviation of the mean hurricane temperatures from the mean tropical sounding.

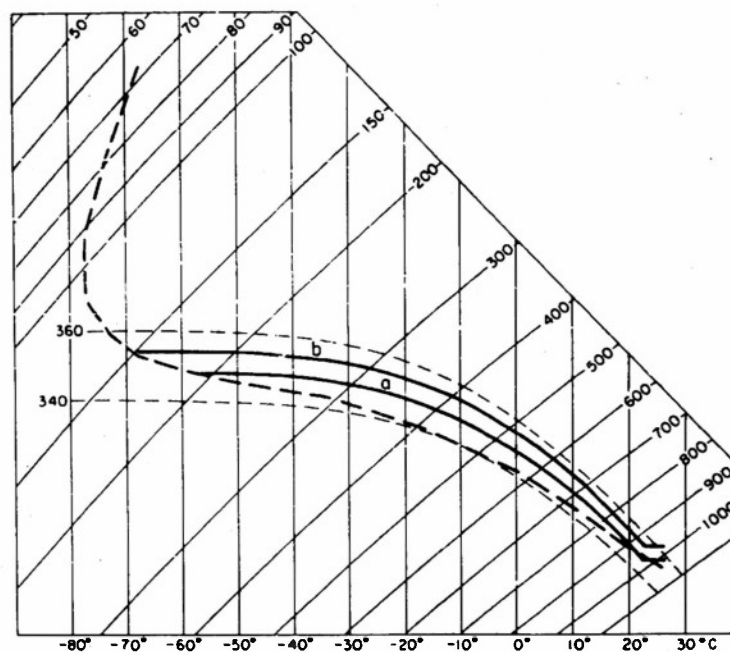


Fig. 6 Tephigram showing the mean tropical atmosphere (dashed) and two adiabatic ascent curves (solid) determined by prescribed values of surface pressure, temperature, and moisture.

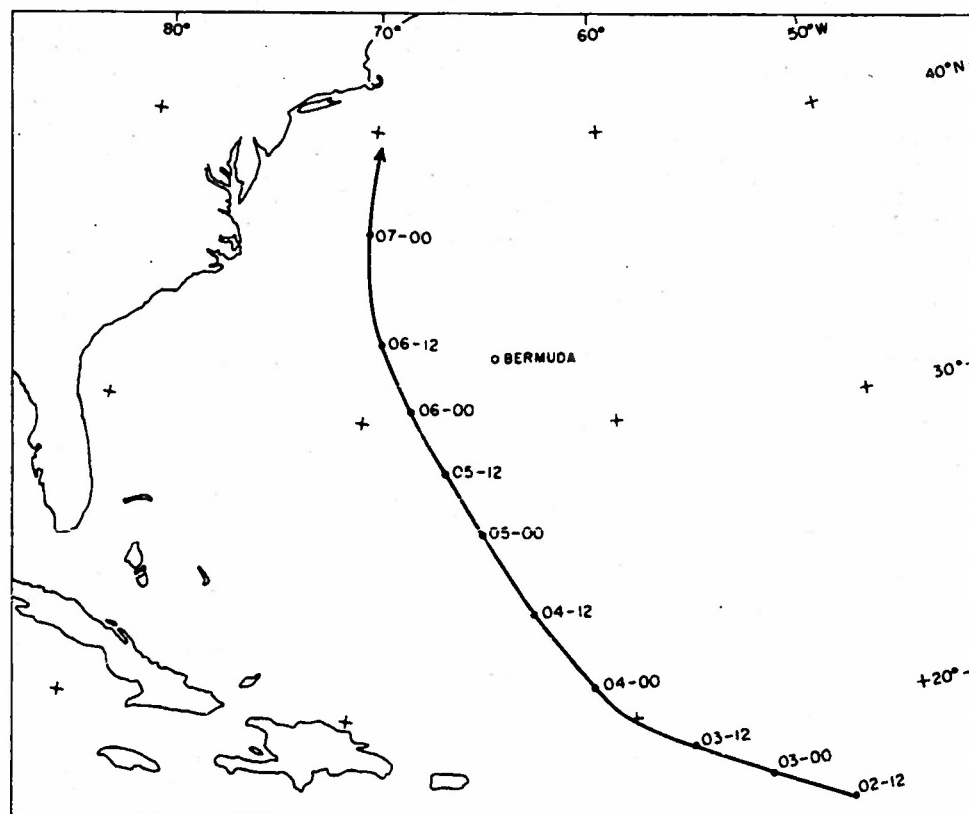


Fig. 7 Track of hurricane, September 2-7, 1953.



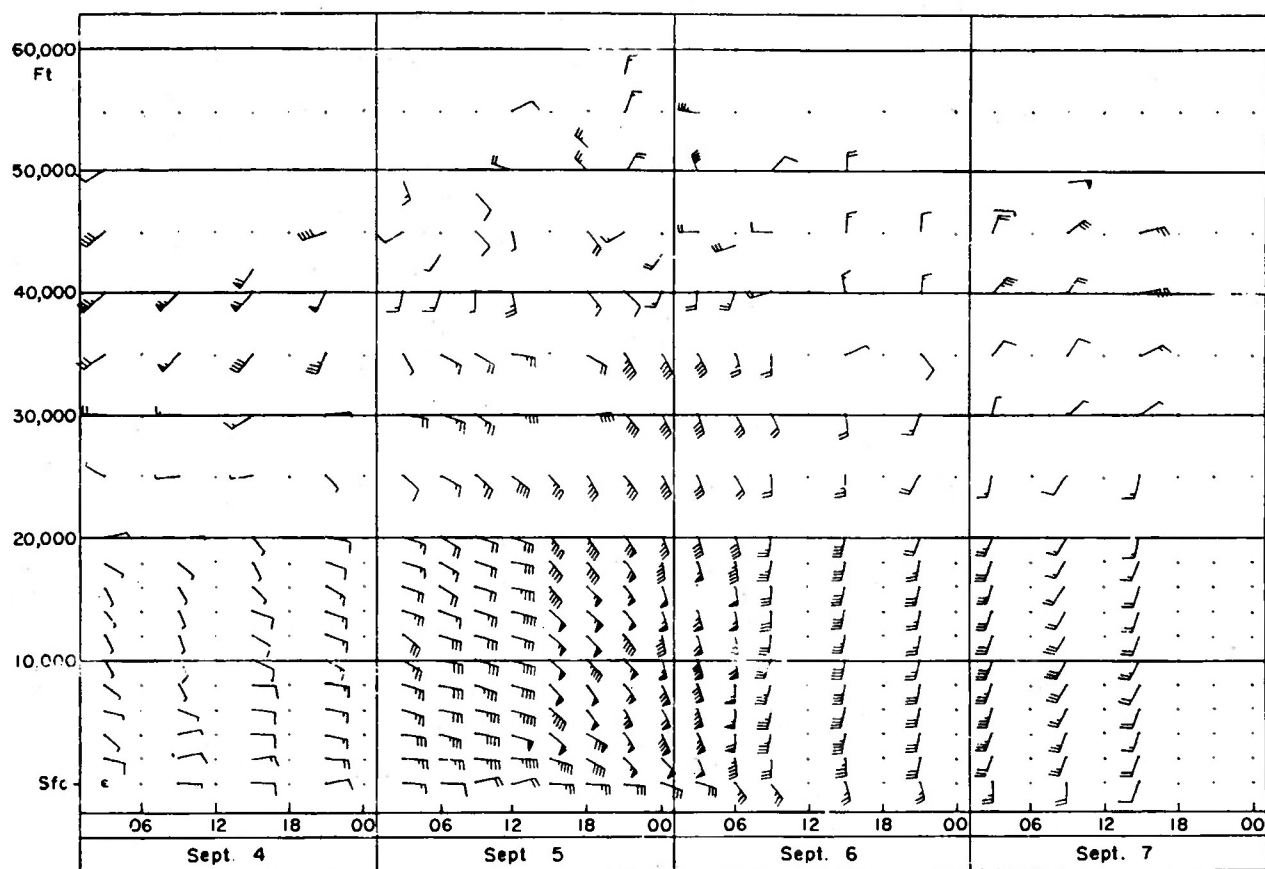


Fig. 8 Time cross section of wind field at Bermuda.  
Wind speeds are in knots.

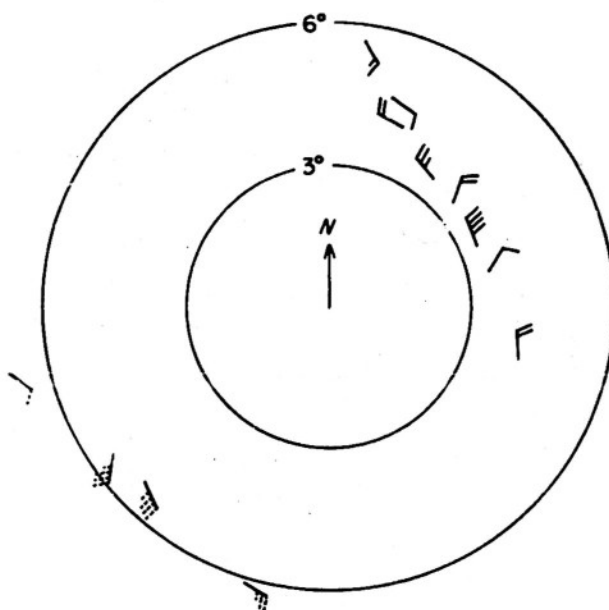


Fig. 9 50,000 ft winds plotted relative to the hurricane center;  
Bermuda (solid) and San Juan (dashed).

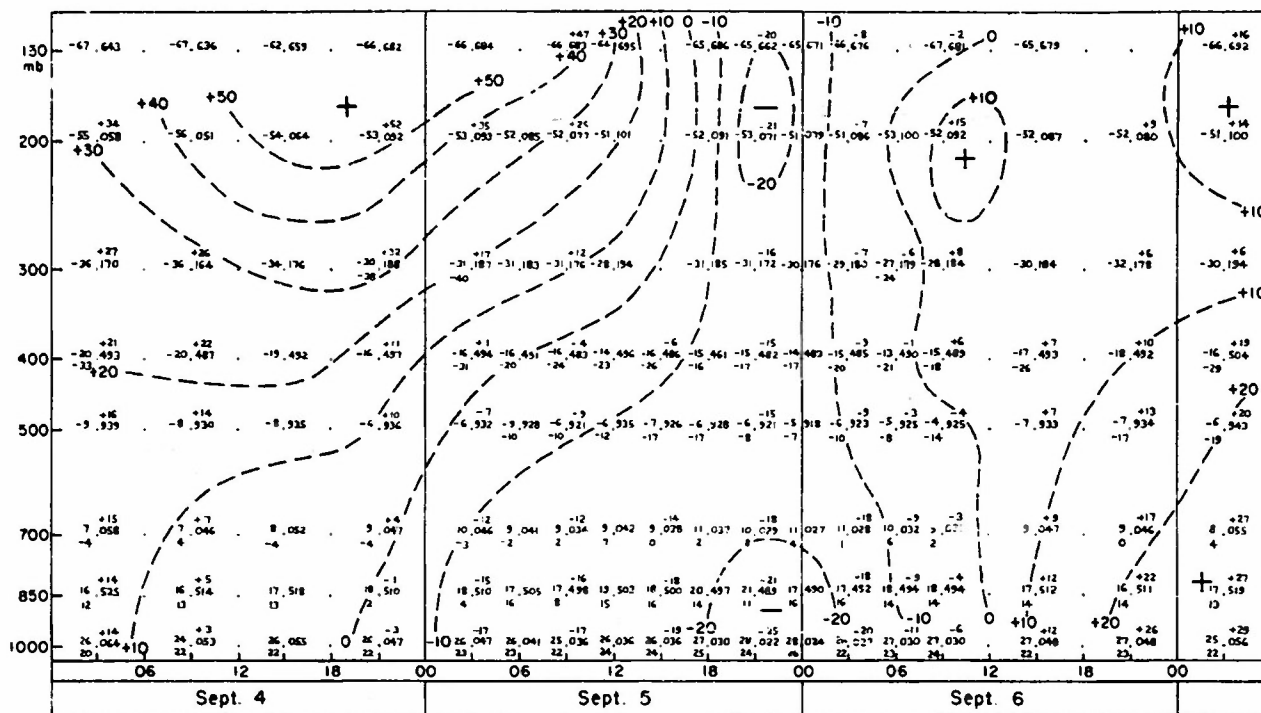


Fig. 10 Time cross section for Bermuda of height, temperature and dew point at standard isobaric surfaces (standard plotting model). The 24-hr height change is plotted above the height value. Dashed lines are isolines of height change in tens of feet.

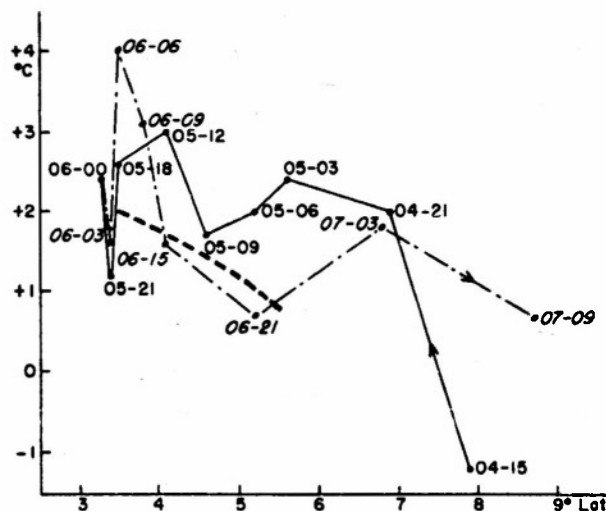


Fig. 11 Deviation of Bermuda 500 - 200 mb mean temperature from mean tropical. Time sequence is shown by light curves; solid as storm approached, dash-dot as the storm moved away. The heavy dashed curve shows the deviations of the mean hurricane soundings from the mean tropical for the same layer.

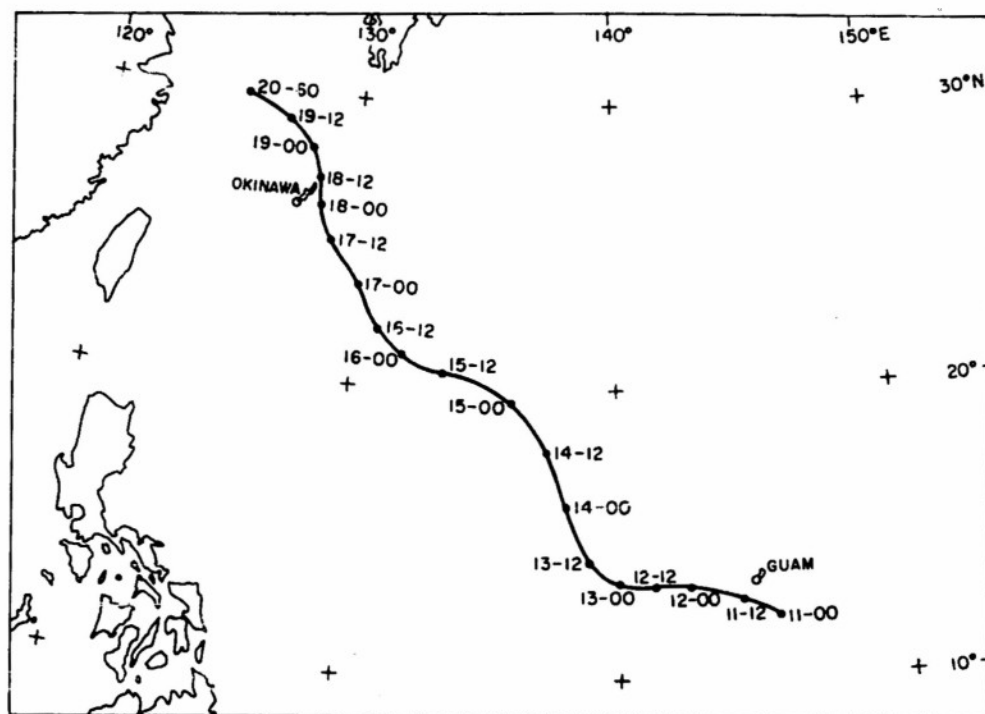


Fig. 12 Track of typhoon August 11 - 20, 1951.

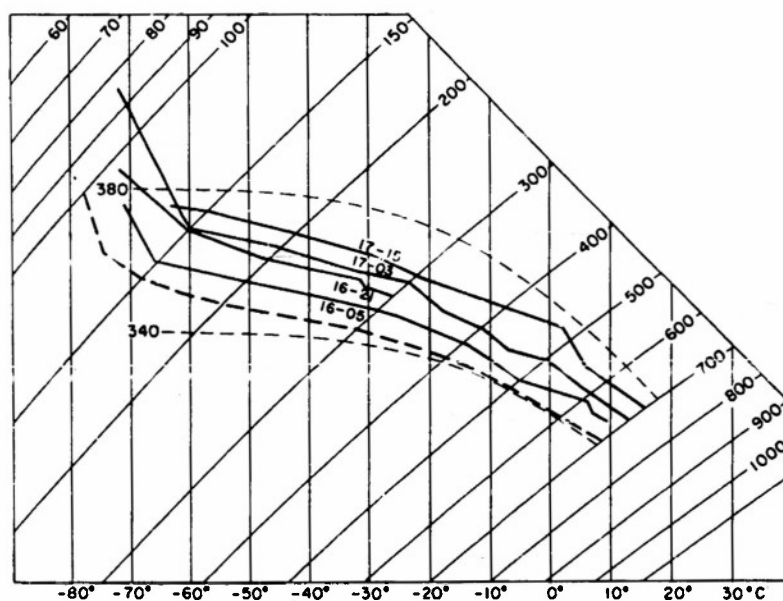


Fig. 13 Tephigram showing upper portion of soundings made at Kadena AFB, Okinawa during August 16 and 17, 1951 (solid) and the mean tropical sounding (dashed).

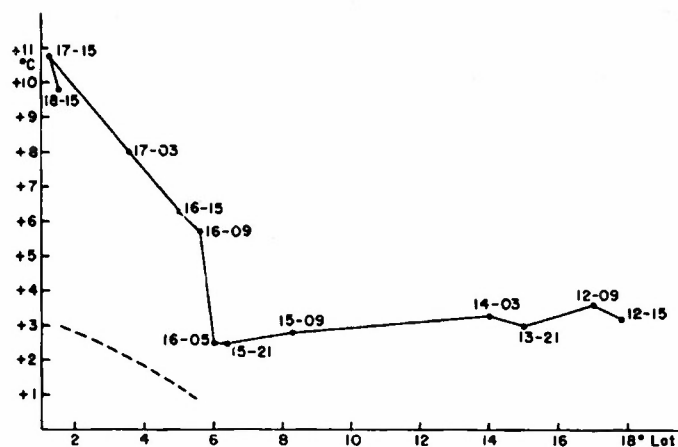


Fig. 14 Deviation of Okinawa 500 - 200 mb mean temperature from mean tropical. Dashed curve shows the deviations of the mean hurricane soundings from the mean tropical for the same layer.

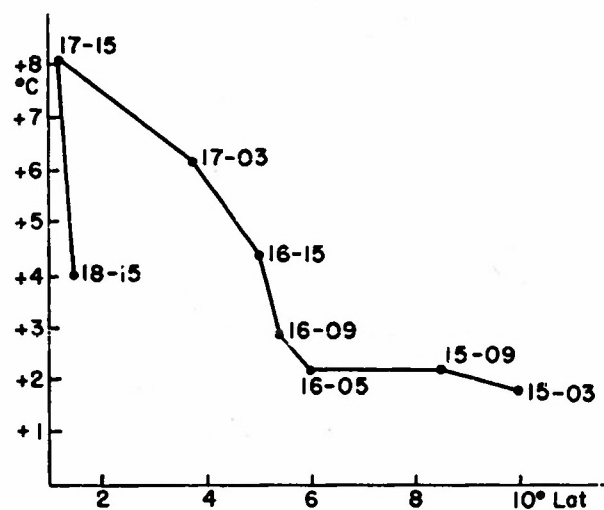


Fig. 15 Deviation of Okinawa 700 - 500 mb mean temperature from mean tropical.

References

- Arakawa, H., 1950: Vertical structure of a mature typhoon. Mon. Wea. Rev., 78, 197-200.
- Haurwitz, B., 1935: The height of tropical cyclones and of the "Eye" of the storm. Mon. Wea. Rev., 63, 45-49.
- Jordan, E. S., 1952: An observational study of the upper wind-circulation around tropical storms. J. Meteor., 9, 340-346.
- Kasahara, A., 1953: A note on the vertical structure of the pressure and temperature fields in a typhoon. J. Meteor. Soc. Japan, 31, 22-35.
- Middleton, W. E. K. and A. F. Spilhaus, 1953: Meteorological Instruments. Univ. of Toronto Press.
- Palmen, E., 1948: On the formation and structure of tropical hurricanes. Geophysica, 3, 26-38.
- Riehl, H., 1951: Aerology of tropical storms. In Compendium of Meteorology, Boston, Amer. Meteor. Soc., 902-913.
- Riehl, H., 1954: Tropical Meteorology. McGraw-Hill, New York.
- Schacht, E., 1946: A mean hurricane sounding for the Caribbean area. Bull. Amer. Meteor. Soc., 27, 324-327.
- Simpson, R. H., 1947: A note on the movement and structure of the Florida hurricane of October 1946. Mon. Wea. Rev., 75, 53-58.
- Simpson, R. H., 1952: Exploring eye of typhoon "Marge" 1951. Bull. Amer. Meteor. Soc., 33, 286-298.

Ship Reports of Cloudiness as an Aid  
in Low Latitude Weather Analysis

by

G. E. Birchfield

The University of Chicago

Abstract

Surface reports from ships can be used to show the synoptic cloud distribution over the tropical oceans. The cloud patterns can be classified into three general types. In two of the three types, the vorticity equation can be used to deduce models of the upper level circulation.

\* \* \*

As generally known it is often difficult to determine the "synoptic" distribution of weather and cloudiness in low latitudes from land reports because of local effects. More representative would be charts showing the distribution of cloudiness over the open sea. For this purpose we must normally rely on ship observations, since frequent and reliable aircraft reports are lacking in most areas. Ship observations, however, usually are not considered very reliable, and the current synoptic code does not contain sufficient types of cumuli to permit adequate reporting of the state of the sky [17]. Nevertheless, since it was the only route open, an experiment was carried out during August and September 1953, to determine just what could be extracted from a detailed analysis of ship data. This experiment was part of a research program carried out by a University of Chicago group at Fleet Weather Central, Miami, Florida, under the auspices of the Office of Naval Research.

Data plotted consisted of total sky cover, cloud types and amount of low clouds. The maps were analyzed in terms of amount of low clouds, and of regions with high clouds. The area covered was the Atlantic Ocean south of 30°N and west of 55°W, the Caribbean Sea and the Gulf of Mexico. Since the density of ship reports was usually insufficient to analyze cloud charts at any particular map time, the data for all four six-hourly reporting periods during one day were combined. The charts thus represented mean conditions over 18 hours. In view of the slow travel of low latitude disturbances this time interval is admissible in most cases.

The results of the experiment were considerably better than anticipated. Although an ideal fit for all observations was not obtained, it proved possible to ascertain the general areas of good and bad weather and intermediate gradients. It was found on some occasions the data at any individual map time were too scattered to permit locating a disturbance. From the collection of a day's reports, however, a distinct region of bad weather was apparent. In general, continuity from one day to the next was reasonable.



Three types of cloud situations appeared to predominate:

1) There were areas with large amounts of cumulus congestus and cumulonimbus accompanied by middle and high cloud sheets. These were associated with "weather" and at times cyclonic flow near the surface. On some occasions, however, the reflection in the surface flow was poor and the regions of cloudiness provided the only warning of the existence of disturbed weather. In the Lesser Antilles the arrival of a wave trough in the easterlies, a disturbance frequently damped at the surface [2], could in some instances, be anticipated best from the cloud charts.

2) A second distinct type consisted of areas of good weather with no middle and high clouds, few cumuli with any vertical development, but occasionally extensive stratocumulus.

3) The third situation can be described only in general terms. Low clouds occur in average amounts, with little vertical development. There are some high clouds. This combination suggests that high level outflow from a disturbance is superimposed on low level convection of small magnitude, with an intermediate dry and stable layer. Radiosonde observations frequently give evidence of such double moist layers. In the stable layer the moisture element is reported "motor boating"; higher up there is a remarkable increase in the dew point.

In addition to outlining the weather distribution, the cloud charts may be used to aid in the analysis of high tropospheric constant pressure or flow charts in regions without upper air data. The only possible approach is to draw models that have a reasonable chance of verification. The cloud chart when used in conjunction with differential thickness analysis between isobaric surfaces provides one way to construct such models.

In bad weather areas, the high tropospheric flow is divergent from mass continuity considerations; in areas described under 2) above, it may be convergent or non-divergent. The divergence may be approximated from vorticity considerations. Experience with weather and cloudiness near Florida and Cuba, where numerous radiosonde and rawin observations exist, has shown that marked suppression of convective activity and high cloudiness are found where the curvature of the contours of the 200-mb surface become markedly more cyclonic or less anticyclonic, looking downstream; this is especially true at the inflow side of a high level cyclone. Bad weather is found under the inverse circumstances, particularly if the curvature of contours on isobaric surfaces also changes from cyclonic to anticyclonic with increasing height. As an illustration, figure 1 is a typical cloudiness chart, for September 23-24, 1953; figure 2 is the 200-mb contour analysis for 0300Z, September 24, 1953. The lack of cloudiness associated with the inflow of an upper cyclone is illustrated in the cell north of the Lesser Antilles. The low northeast of the Panama Isthmus appears as an area with reduced cloudiness. The large areas of bad weather across the Gulf and Caribbean are associated with the large anticyclone centered over western Cuba.

These observations suggest that Rossby's vorticity theorem [3] can be used as an aid in constructing high level charts in the trade wind belt. If we assume slow local changes with time, as supposed by the construction of cloud charts over a 24-hour interval, we may write the theorem in its steady state form. Using a natural (s, n) system of coordinates,

$$V \frac{\partial}{\partial s} (\zeta + f) + w \frac{\partial}{\partial z} (\zeta + f) = -(\zeta + f) \text{div}_H V, \quad (1)$$

where  $V$  and  $w$  are the horizontal and vertical wind components,  $f$  is the Coriolis parameter,  $\text{div}_H V$  the horizontal divergence,  $K$  the streamline curvature, and  $\zeta = KV - \partial V / \partial n$  is the relative vorticity. We shall assume that the absolute vorticity is positive, that the curvature of the contours and streamlines on an upper isobaric surface have the same sign, and that the relative vorticity appears mainly as curvature.

In areas of suppressed convection with few or no upper clouds the settling motion is slow so that one may consider the motion as quasi-horizontal. Taking an area of no high clouds and no large vertical development as evidence of convergence around the 200-mb level, with slow subsidence, then eq. (1) states that the absolute vorticity increases downstream. This increase will show up as increasing cyclonic curvature of the streamlines if the change takes place in a latitude interval small enough so that the variation of the Coriolis parameter may be neglected.

In an area of extensive cumulonimbus clouds the ascending motion is sufficiently rapid that the vertical gradient of vorticity becomes significant in spite of subsidence between clouds. It is found from observations that frequently the vertical term is the most important. Assuming that this term is at least of the same order of magnitude as the horizontal term in such an area of convergence, the absolute vorticity will increase with height, in addition to increasing downstream horizontally, up to the level of non-divergence, where a maximum is reached. In the upper troposphere, with divergence around 200-mb, we have decreasing absolute vorticity and decreasing cyclonic curvature of streamlines with altitude. Thus, in an area of large scale vertical development of cumulus clouds, the absolute vorticity at first increases from the surface upward and streamlines and contours become more cyclonic; higher up the absolute vorticity decreases with height and streamlines and contours become more anticyclonic.

If there is some definite evidence of the existence of an upper shear line or jet stream, the preceding discussion may be modified to include also the horizontal shear of the wind.

It must be said that the association between cloudiness and the gradient of contour curvature as described is not without exception. But the model verifies with sufficient frequency that by and large better 200-mb charts are likely to be drawn with its use than without any model at all. It is therefore suggested that lacking data, 200-mb contours in the trades be drawn so that (1) the absolute vorticity, as given by contour curvature and Coriolis parameter, will in general increase and certainly not decrease downstream along the contours in regions with suppressed convection, and that (2) the contour curvature will become less cyclonic or more anticyclonic with increasing height in zones of organized convection; preferably the absolute vorticity should also decrease and certainly not increase downstream along the 200-mb contours.

### Acknowledgement

The analysis of the cloudiness charts was made under the direction of Dr. Herbert Riehl. His further assistance in the preparation of this report is gratefully acknowledged.

### References

1. Riehl, H. "Tropical Meteorology," New York: McGraw-Hill Book Co., 1954.
2. Riehl, H., 1945: "Waves in the Easterlies and the Polar Front in the Tropics," Dept. Meteor., Univ. Chicago, Misc. Rep. No. 17.
3. Rossby, C.-G and collaborators, 1939: "Relations between Variations in the Intensity of the Zonal Circulation of the Atmosphere and the Displacement of the Semipermanent Centers of Action," J. Mar. Res. 2, 38-55.

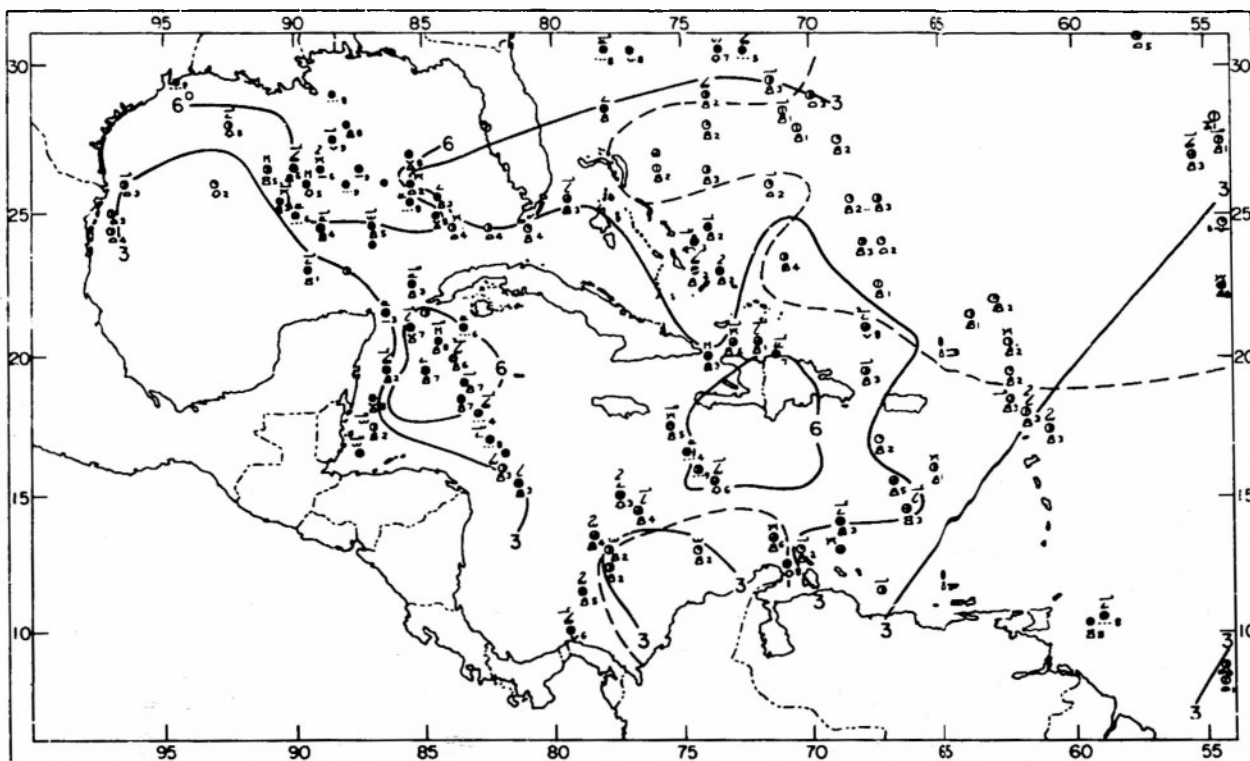


Fig. 1. Cloudiness map for the period 1200Z, Sept. 23 to 1200Z, Sept. 24, 1953. Amount of low clouds is in synoptic code figures, e.g. code figure 3 corresponds to 4 tenths, code figure 6 to 7-8 tenths. Dashed lines separate areas reporting high clouds from areas without high clouds.

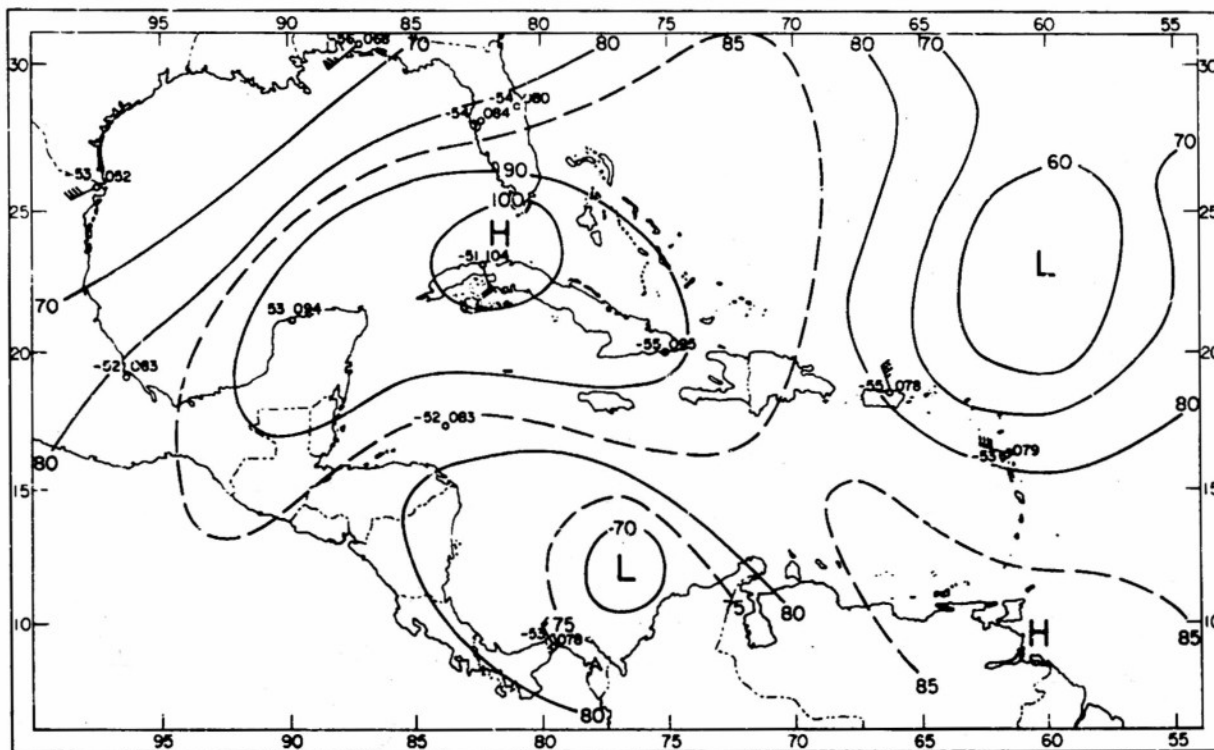


Fig. 2. 200-mb chart for Sept. 24, 1953, 0300Z, for the Caribbean area. Analyzed in hundreds of feet, first digit omitted.